GEOPHYSICAL RESEARCH LETTERS, VOL. 35, L14807, doi:10.1029/2008GL033204, 2008

Click Here for Full Article

# Simulated climate near steep topography: Sensitivity to numerical methods for atmospheric transport

G. Bala,[1,2] R. B. Rood,[3] D. Bader,[1] A. Mirin,[1] D. Ivanova,[1] and Cedric Drui[3]

Received 7 January 2008; revised 23 May 2008; accepted 23 June 2008; published 22 July 2008.

[1] We present the sensitivity of the simulated climate near steep topographical regions when the numerical method for atmospheric transport in the Community Climate System Model (CCSM3) is changed from spectral to a finite volume (FV) transport. Our analysis of the circulation and precipitation shows significant local improvement in three aspects: 1) The Gibbs oscillations present in the cloudiness and shortwave radiative forcing fields in the spectral simulation are absent in the FV simulation. 2) The along-shore component of wind stress in the western coastal regions of North and South America increases in the FV simulation. This tends to reduce the persistent biases in sea surface temperature through enhanced oceanic upwelling. 3) The FV simulation shows improvement in the wet-dry contrast of orographically forced precipitation. These local improvements have impact on continental and larger scales and are critical to the confident use of information from climate predictions in adaptation to climate change.
**Citation:** Bala, G., R. B. Rood, D. Bader, A. Mirin, D. Ivanova, and C. Drui (2008), Simulated climate near steep topography: Sensitivity to numerical methods for atmospheric transport, *Geophys. Res. Lett.*, *35*, L14807, doi:10.1029/2008GL033204.

## 1. Introduction

[2] In a recent study, *Bala et al.* [2008] documented the sensitivity of the global climate as simulated by the Community Climate System Model (CCSM3) [*Collins et al.*, 2006a] when the numerical method for atmospheric transport was changed from a spectral [*Williamson*, 1983; *Williamson and Rasch*, 1994] to a finite volume (FV) transport method [*Lin*, 2004; *Lin and Rood*, 1996, 1997]. In the spectral methods, global basis functions are used to represent the spatial structure of the variables and hence information from both upstream and downstream influences a particular point in space. The FV scheme is upwind biased which reduces dispersion errors.

[3] While the two schemes resolve the large spatial scales accurately, they differ in their treatment of the smaller scales. The use of global basis functions in the spectral methods leads to Gibbs oscillations near sharp spatial gradients. This manifests as ripples near steep topography and frontal zones, and diffusive filters are used to remedy this effect. The FV algorithms implemented in CCSM3 [*Lin*, 2004] - a finite volume scheme for horizontal discretization, piece-wise linear treatment of the pressure gradient term [*Lin*, 1997], and a Lagrangian control-volume treatment in the vertical - are designed to reduce discretization errors in the smallest scales represented by the model. These algorithms are expected to improve the simulation of localized circulations near steep topography when compared to the spectral scheme.

[4] This paper is second in a series of papers that investigate the improvements in long term CCSM3 simulations due to a change in numerical methods from the spectral to the FV methods. *Bala et al.* [2008] reported the fidelity of the climate simulations from a global climate perspective. Improvements in the simulated wind stress, sea surface temperatures, oceanic transport in the Antarctic Circumpolar Current and the seasonal cycle of sea ice in the Arctic and Antarctic were documented. The Arctic sea ice thickness distribution was also improved, with thicker ice along the Canadian coast and thinner ice in the East Siberian Sea. Especially in the summertime, the simulated atmospheric circulation in the Arctic was more consistent with observations.

[5] From a global climate perspective, these improvements were minor. However, there are many features of climate which are local in their determination. Topographical regions where the spatial gradients are strong would be the obvious place to look for the anticipated improvements in smaller scales. In this paper, we investigate in some detail the sensitivity of the spatial patterns of wind stress, precipitation, clouds and radiative forcing near steep topography to changes in the numerical formulation for the atmospheric dynamics.

## 2. Model and the Simulations

[6] CCSM3 is the third generation NCAR/DOE coupled atmosphere-ocean model. CCSM3 has the following model components: The Community Atmosphere Model version 3 (CAM3) [*Collins et al.*, 2006b, 2006c], the Community Land Surface Model version 3 (CLM3) [*Dickinson et al.*, 2006], the Community Sea Ice Model version 5 (CSIM5) [*Briegleb et al.*, 2004], and the Parallel Ocean Program version 1.4.3 (POP) [*Smith and Gent*, 2004].

[7] For the simulations presented here, we use the Finite Volume (FV) method for the atmospheric component at a horizontal resolution of 1 degree in latitude and 1.25 degrees in longitude [*Bala et al.*, 2008]. This configuration is referred to as FVx1. Our simulation is a 400 year present-day control simulation and it will be compared to a corresponding 700-year T85 present-day control simulation performed at NCAR [*Collins et al.*, 2006a]. This FVx1

[1]Lawrence Livermore National Laboratory, Livermore, California, USA.
[2]Now at Center for Atmospheric and Oceanic Sciences, Indian Institute of Science, Bangalore, India.
[3]Department of Atmospheric, Oceanic and Space Sciences, University of Michigan, Ann Arbor, Michigan, USA.


0094-8276/08/2008GL033204$05.00

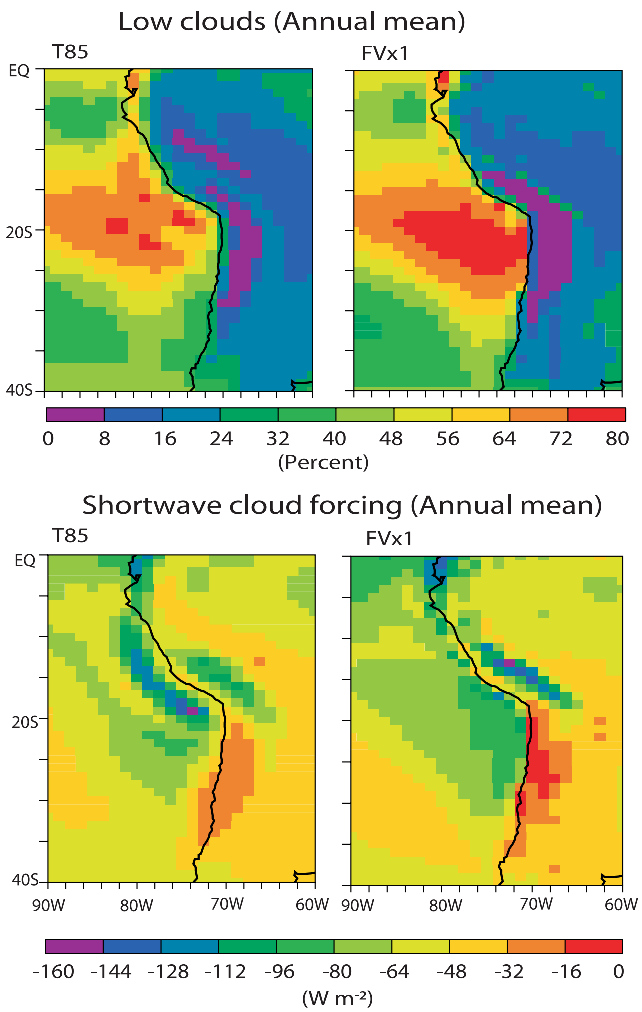


**Figure 1.** (top) Annual-mean low clouds and (bottom) shortwave cloud radiative forcing in the eastern Pacific Ocean in the CCSM3 T85 and FVx1 simulations. The Gibbs oscillation, which manifests as alternating minima and maxima in marine stratus clouds and shortwave cloud radiative forcing offshore of South America in the T85 simulation, is not present in the FVx1 simulation.

configuration necessitated slight retuning of the parameters of the cloud and convection parameterization in the model, changes to the terrain filter algorithm (adoption of a monotonic filter; S.J. Lin, personal communication), and a change in the ocean viscosity formulation [*Bala et al.*, 2008; *Jochum et al.*, 2008].

## 3. Results

[8] In this section, we investigate the model simulations near the west coasts of the continents, where steep topography is important. The mean climate produced by FVx1 is represented by the average over years 300–399. We compare it to the T85 mean climate represented by the average over years 600–699. The drift in the mean quantities is sufficiently small that they do not significantly impact the comparison [*Bala et al.*, 2008].

### 3.1. Low-Level Clouds and Radiation

[9] Near steep topography spectral simulations exhibit Gibbs oscillations. To reduce these spurious oscillations, spectral models use smoothed topography [e.g., *Navarra et al.*, 1994] which reduces the resolution of the topography and could be detrimental to the fidelity of simulated regional climate. The terrain filter in the spectral method itself may generate Gibbs oscillations in the terrain field. The Gibbs oscillations in the annual mean low level clouds are visually evident with T85 (Figure 1, top left) in the area of high cloudiness west of the South America coast where the FVx1 simulation shows a more homogeneous region of high cloudiness (Figure 1, top right). There are also visible differences over land. These differences in clouds lead to large differences in the shortwave cloud radiative forcing (Figure 1, bottom). The differences in the radiative forcing are, in places, greater than 40 $Wm^{-2}$. These large differences are in patterns which are persistent. *Wielicki et al.* [2002] have shown from observations that significant variability occurs at a magnitude of $\sim$2 $Wm^{-2}$, and that climate models do not represent variability of cloud radiative forcing. The removal of these spatially coherent, stationary errors is a necessary step in addressing the model errors [*Wielicki et al.*, 2002].

### 3.2. Wind Stress and SST

[10] Near the western coastal regions of the continents, a weak equatorward, alongshore component of wind stress has been a persistent bias in CCSM. The along-shore component is responsible for the upwelling of cold water along the west coast of continents [*Large and Danabasoglu*, 2006]. Warmer SST biases in the western coastal regions in earlier CCSM simulations have been attributed to weaker along-shore wind stress and the associated weaker upwelling [*Collins et al.*, 2006a].

[11] The FVx1 simulation exhibits systematic improvement when compared to T85 with respect to the low level dynamical circulation (Figure 2). The annual mean surface wind stress and the SST differences in the ocean basins west of North and South America show that the along-shore equatorward wind stress is stronger in the FVx1 simulation relative to the T85 simulation (Figure 2). Since this component is larger in the FVx1 simulation, there is more upwelling and the SSTs are colder in the FVx1 simulation. The cooler SSTs in FVx1 are statistically significant at the 1% level. The wind stress magnitude differences are also significant at the 1% level in these regions [*Bala et al.*, 2008]. Improvements in the along-shore wind stress were also obtained in CAM3 when the model resolution was increased from T42 to T85 [*Hack et al.*, 2006], suggesting that increasing the model resolution also helps to reduce the circulation bias near steep topographical regions.

[12] The equatorward component of the wind stress in FVx1 has decreased compared to T85 in southern Africa. Consequently, warm SST bias has increased near South Africa in FVx1. Compared with North and South America, the large-scale atmospheric dynamics in southern Africa are not as prominently influenced by topography. The deficiencies in this region, therefore, are related to deficiencies in large-scale atmospheric and oceanic dynamics.

[13] The warm SST bias in the ocean basins west of North America, South America and South Africa has been

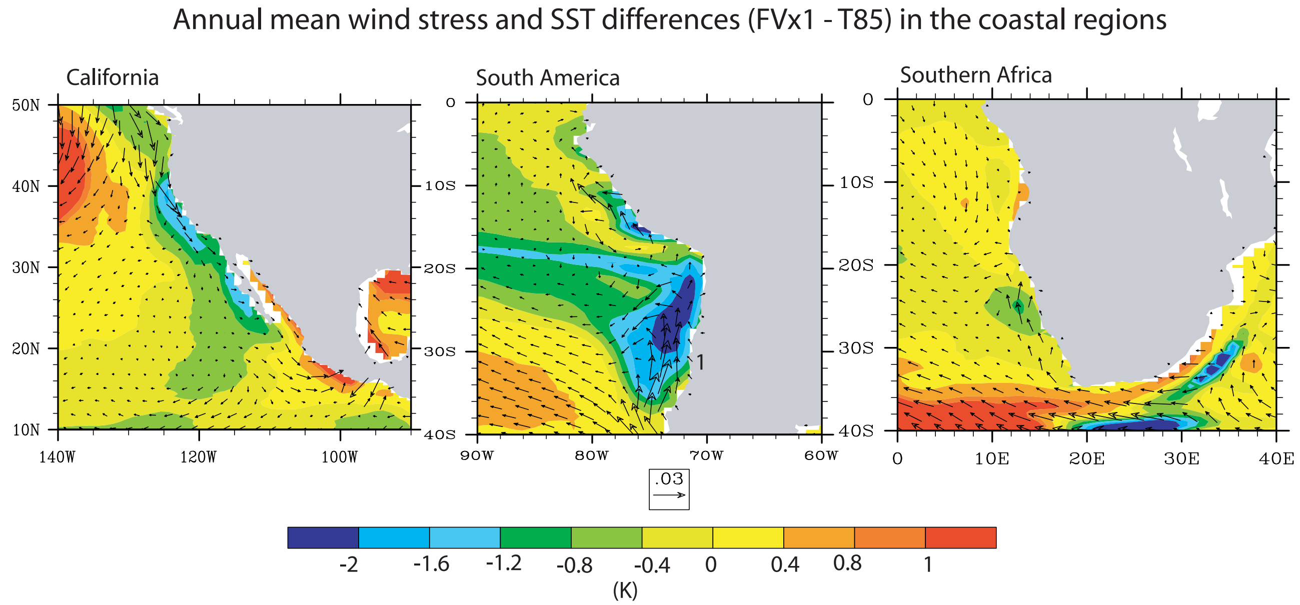


**Figure 2.** Differences in annual-mean wind stress (N m$^{-2}$), and SST between CCSM3 FVx1 and T85 simulations. The along-shore component of the surface wind stress increases in the FVx1 simulation, which tends to increase the upwelling along the coasts and to reduce the warmer sea surface temperature bias in the T85 simulation.

previously attributed to a persistent deficiency of marine stratocumulus clouds in these regions [*Collins et al.*, 2006a]. The lower amounts of marine clouds in turn lead to less (in magnitude) annual mean shortwave cloud radiative forcing in these coastal regions. The reduction of the warm SST bias in FVx1 leads to increased annual mean low level clouds, and an increase in the magnitude of shortwave cloud forcing when compared to the T85 simulation (Figure 3). The improvements in the treatment of the small scales by the numerical algorithm can provide a better path toward the development of improved parameterizations. In the case of benefits that might be realized by increased resolution in the spectral model [e.g., *Hack et al.*, 2006], the Gibbs oscillation can largely mask the improvements in places of steep topography (e.g. South America in Figures 1 and 3).

### 3.3. U.S. Precipitation

[14] The impact of the numerical formulation on precipitation near steep topographical regions is assessed in Figure 4, which compares January-mean precipitation fields in the United States to observed National Oceanic and Atmospheric Administration [*National Oceanic and Atmospheric Administration*, 2003] precipitation. The NOAA dataset is on a quarter degree grid. In both January and July (figure not shown), the precipitation in the eastern half of the United States, where topography is not a dominant effect, is similar in the two simulations. In January in the western United States, when precipitation is dominated by synoptic-scale orographic effects, there are significant differences between the two simulations. Of note, the observed minimum in Oregon and Washington and the separation of the precipitation in the Cascade (Oregon and Washington) and Rocky Mountains (Idaho and Montana) are absent in the T85 simulation but can be seen in the FVx1 simulation. To the east, the precipitation associated with the mountains in Wyoming and Colorado is emerging in the FVx1 simulation. The much narrower rain-shadow in the Central Valley of California is not simulated in either simulation. However, the distinct orientation of the Sierra Nevada Mountains is appearing in the FVx1 simulation, with much more contrast between the dry areas both upstream (west of) and downstream (east of) these mountains. In the T85 simulation there is much more precipitation in deserts of Nevada and Utah than in the FVx1 simulation.

[15] In high resolution simulations with the spectral dynamical core in the Community Atmosphere Model [*Iorio et al.*, 2004], the precipitation associated with the mountain ranges in Wyoming and Colorado appears only when the resolution is increased to T170 or higher. The lack of separation of the precipitation associated with the Cascades and the Rocky Mountains in the northwest United States is a persistent feature at resolutions as high as T239. There is also a persistent wet anomaly to the east of the Sierra Nevada in Nevada and Utah. In atmospheric-model-only simulations we have performed with the FV method, all of these western United States features are better represented as resolution is increased. This means that the wet-dry contrast important for regional water resources is better represented with the FV method. This improvement is also partly attributable to the higher spatial resolution in the FVx1 simulation relative to the T85 simulation ($1° \times 1.25°$ vs. $1.4° \times 1.4°$).

[16] The terrain filter (for the FVx1 simulation) is a monotonic filter that removes the non-resolvable two-delta-grid-length terrain structures without creating new peaks or valleys. In order to assess the impact of this filter, we compared the precipitation patterns from a CAM3 FVx1 AMIP (Atmospheric Model Intercomparison Project) simulation that uses the monotonic filter to another CAM3 FVx1 AMIP simulation that uses the spectral filter. The rain-shadow features are present in both simulations, though the maximum rainfall at peak elevations is reduced by 50% in the simulation with spectrally filtered topography. This indicates that the simulated pattern of the wintertime pre-

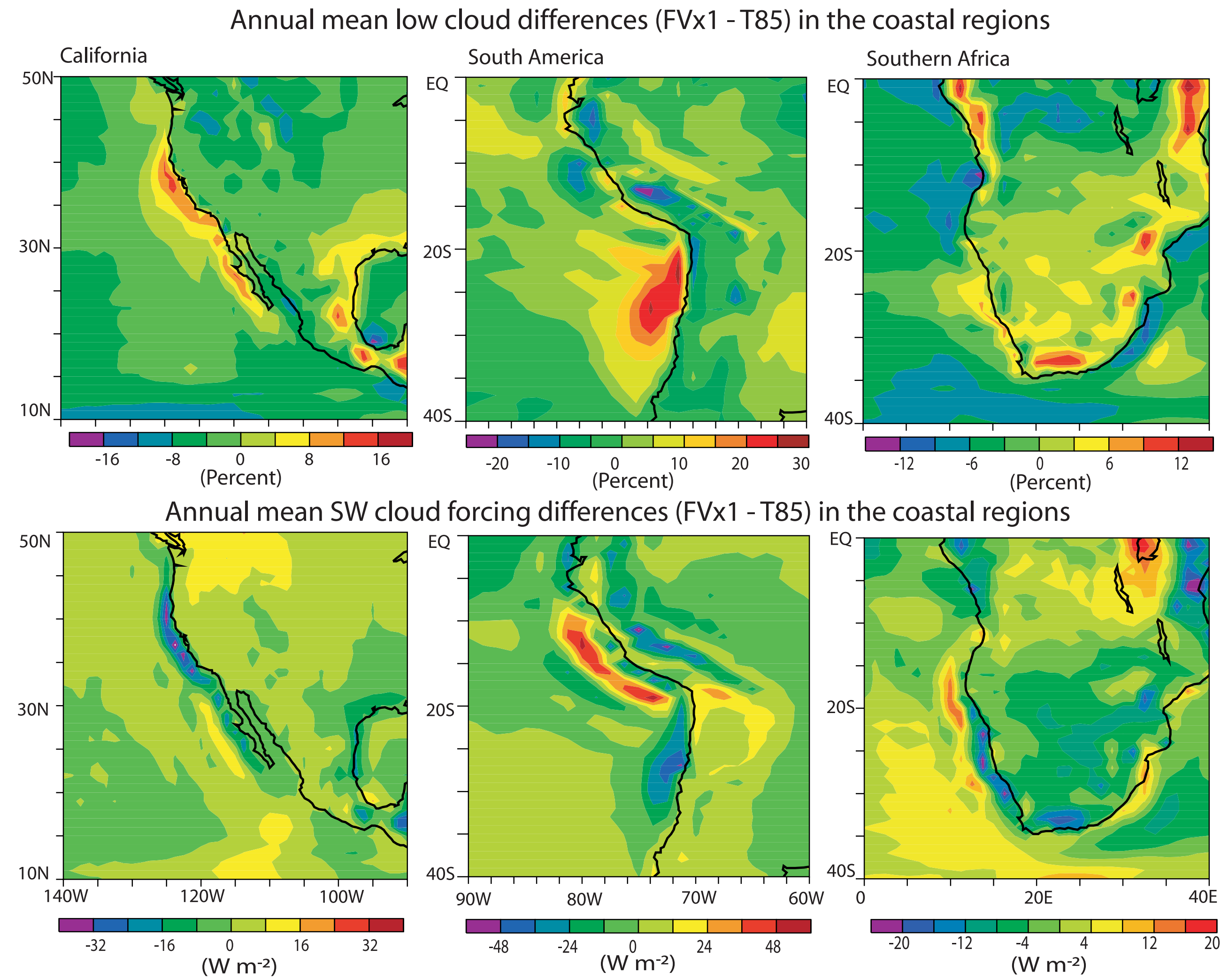


**Figure 3.** Differences in (top) annual-mean low clouds and (bottom) shortwave cloud radiative forcing between CCSM3 FVx1 and T85 in the western coastal regions. The cooler sea surface temperatures in the FVx1 simulation tend to increase the low clouds and increase the magnitude of the shortwave cloud radiative forcing in these coastal regions.

cipitation is sensitive to the filtering techniques used for the topography, and implies that topographical filtering should be considered part of the dynamical core.

## 4. Discussion

[17] In an earlier paper [*Bala et al.*, 2008], comparisons of the FVx1 and T85 simulations from a global climate perspective were presented. Statistically significant improvements were noted in the simulation of the global surface wind stress which resulted in reduced errors in the simulated sea surface temperature, sea ice extent and thickness distributions. From a global climate perspective, these improvements were minor; quantitative comparison demonstrated that the simulated climate of the FV version of the CCSM coupled model was very similar to that of the T85 version in terms of its biases.

[18] This paper shows that local quantities near steep topography are strongly influenced by the numerical formulation. Some of the improvements noted are directly related to the elimination of the spurious ripples associated with the spectral method. This verifies that monotonicity constraints, often cited as important for tracer transport, are important to the representation of resolved dynamics in general. Other benefits are realized because the improved representation of local dynamics directly benefits the representation of parameterized physical processes.

[19] These local changes can have significant meaning for continental-scale climate. For example, local processes are ultimately at the foundation of the mechanisms that transport moisture into the interior of the continents. In other instances, the improvements here are necessary, but not sufficient, to address large-scale biases in climate models. For example, *Wielicki et al.* [2002] note major deficiencies in all climate models in their representation of tropical variability of cloud-radiative forcing. The removal of persistent, spurious features such as those documented here is a step towards allowing the representation of local dynamical features that are important for larger scale variability.

[20] Finally, this paper focused on the impact near steep topography. There are a number of other sharply defined features that are expected to benefit from a more local representation of the dynamics. These include land-sea

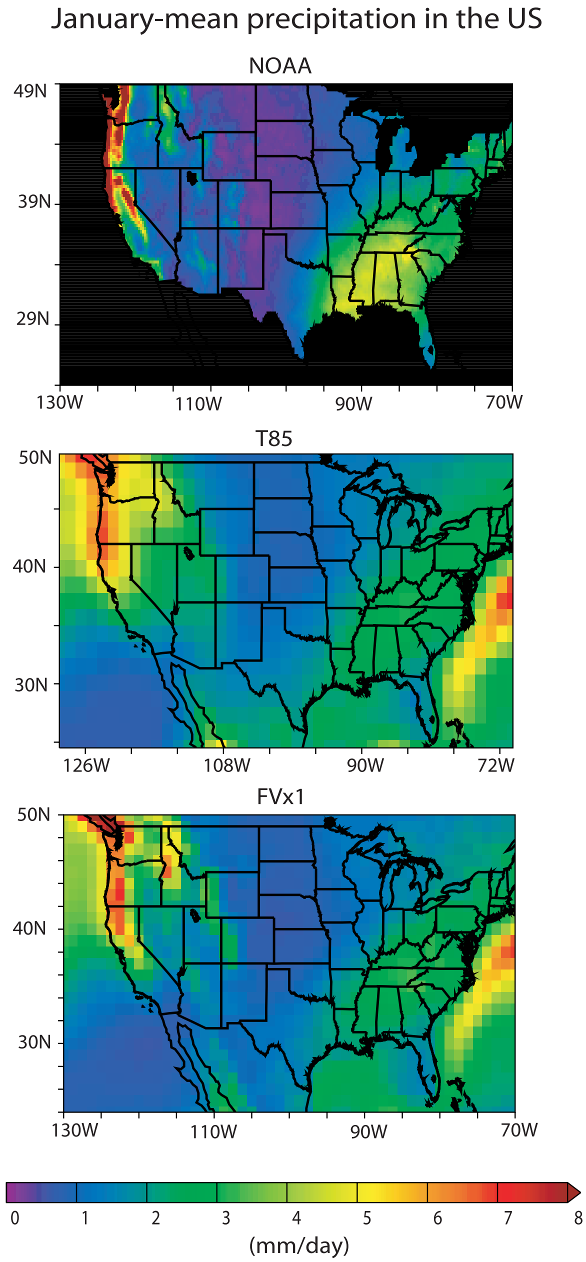


**Figure 4.** Precipitation over the continental United States in January from (top) observations, (middle) CCSM3 T85, and (bottom) FVx1 simulations. The rain-shadow features in Oregon and Washington that are absent in the T85 simulation can be seen to emerge in the FVx1 simulation. Further, the wet bias of the T85 simulation in Nevada and Utah is reduced in FVx1.

circulations that are expected to be important to, for instance, precipitation in the eastern United States; the often sharply defined edges of deserts and how deserts may change as the climate warms; and processes near the tropopause. Representation of these features requires higher resolution than presented here.

[21] **Acknowledgments.** This work was performed under the auspices of the U.S. Department of Energy Lawrence Livermore National Laboratory under contract DE-AC52-07NA27344.

## References

Bala, G., R. B. Rood, A. Mirin, J. McClean, K. Achutarao, D. C. Bader, P. J. Gleckler, R. Neale, and P. J. Rasch (2008), Evaluation of a CCSM3 simulation with a finite volume dynamical core for the atmosphere at 1° latitude × 1.25° longitude resolution, *J. Clim.*, *21*, 1467–1486.

Briegleb, B. P., C. M. Bitz, E. C. Hunke, W. H. Lipscomb, M. M. Holland, J. L. Schramm, and R. E. Moritz (2004), Scientific description of the sea ice component of the Community Climate System Model version 3, *Tech. Rep. NCAR/TN-463+STR*, 78 pp., Natl. Cent. for Atmos. Res., Boulder, Colo.

Collins, W. D., et al. (2006a), The Community Climate System Model version 3 (CCSM3), *J. Clim.*, *19*, 2122–2143.

Collins, W. D., P. J. Rasch, B. A. Boville, J. J. Hack, J. R. McCaa, D. L. Williamson, B. P. Briegleb, C. M. Bitz, S. J. Lin, and M. H. Zhang (2006b), The formulation and atmospheric simulation of the Community Atmosphere Model version 3 (CAM3), *J. Clim.*, *19*, 2144–2161.

Collins, W. D., et al. (2006c), Description of the NCAR Community Atmosphere Model (CAM 3.0), *Tech. Note NCAR/TN-464+STR*, 214 pp., Natl. Cent. for Atmos. Res., Boulder, Colo.

Dickinson, R. E., K. W. Oleson, G. Bonan, F. Hoffman, P. Thornton, M. Vertenstein, Z. L. Yang, and X. B. Zeng (2006), The Community Land Model and its climate statistics as a component of the Community Climate System Model, *J. Clim.*, *19*, 2302–2324.

Hack, J. J., J. M. Caron, G. Danabasoglu, K. W. Oleson, C. Bitz, and J. E. Truesdale (2006), CCSM-CAM3 climate simulation sensitivity to changes in horizontal resolution, *J. Clim.*, *19*, 2267–2289.

Iorio, J. P., P. B. Duffy, B. Govindasamy, S. L. Thompson, M. Khairoutdinov, and D. Randall (2004), Effects of model resolution and subgrid-scale physics on the simulation of precipitation in the continental United States, *Clim. Dyn.*, *23*, 243–258.

Jochum, M., G. Danabasoglu, M. M. Holland, Y.-O. Kwon, and W. G. Large (2008), Ocean viscosity and climate, *J. Geophys. Res.*, *113*, C06017, doi:10.1029/2007JC004515.

Large, W. G., and G. Danabasoglu (2006), Attribution and impacts of upper-ocean biases in CCSM3, *J. Clim.*, *19*, 2325–2346.

Lin, S. J. (1997), A finite-volume integration method for computing pressure gradient force in general vertical coordinates, *Q.J.R. Meteorol. Soc.*, *123*, 1749–1762.

Lin, S. J. (2004), A "vertically Lagrangian" finite-volume dynamical core for global models, *Mon. Weather Rev.*, *132*, 2293–2307.

Lin, S. J., and R. B. Rood (1996), Multidimensional flux-form semi-Lagrangian transport schemes, *Mon. Weather Rev.*, *124*, 2046–2070.

Lin, S. J., and R. B. Rood (1997), An explicit flux-form semi-Lagrangian shallow-water model on the sphere, *Q.J.R. Meteorol. Soc.*, *123*, 2477–2498.

Navarra, A., W. F. Stern, and K. Miyakoda (1994), Reduction of the Gibbs oscillation in spectral model simulations, *J Clim.*, *7*, 1169–1183.

National Oceanic and Atmospheric Administration (2003), CPC US unified (0.25° × 0.25°) precipitation, http://www.cdc.noaa.gov/cdc/data.unified.html, NOAA-CIRES Clim. Diagn. Cent., Boulder, Colo.

Smith, R. D., and P. R. Gent (2004), Reference manual for the Parallel Ocean Program (POP), ocean component of the Community Climate Model (CCSM2.0 and 3.0), *Tech. Rep. LA-UR-02-2484*, Los Alamos Natl. Lab., Los Alamos, N.M. (Available online at http://www.ccsm.ucar.edu/models/ccsm3.0/pop.)

Wielicki, B. A., et al. (2002), Evidence for large decadal variability in the tropical mean radiative energy budget, *Science*, *295*, 841–844.

Williamson, D. L. (1983), Description of NCAR Community Climate Model (CCM0B), *Tech. Rep. NCAR/TN-210+STR*, 88 pp., Natl. Cent. for Atmos. Res., Boulder, Colo.

Williamson, D. L., and P. J. Rasch (1994), Water vapor transport in the NCAR-CCM2, *Tellus A*, *46*, 34–51.

D. Bader, D. Ivanova, and A. Mirin, Lawrence Livermore National Laboratory, 7000 East Avenue, Livermore, CA 94550, USA.

G. Bala, Center for Atmospheric and Oceanic Sciences, Indian Institute of Science, Bangalore, 560 012, India.

C. Drui and R. B. Rood, Department of Atmospheric, Oceanic and Space Sciences, University of Michigan, 2455 Hayward Street, Ann Arbor, MI 48109, USA. (rbrood@umich.edu)